



Structural modification of mordenite zeolite with Fe For the photo-degradation of EDTA

Mostafa M. Emara^a, Amal S.M. Tourky^b, Medhat M. El-Moselhy^{a,*}

^a Chemistry Department, Faculty of Science (boys), Al-Azha University, Nasr city 11884, Cairo, Egypt

^b Chemistry Department, Faculty of Science (Girls), Al-Azhar University, Nasr city, Cairo, Egypt

ARTICLE INFO

Article history:

Received 21 September 2008

Received in revised form

14 November 2008

Accepted 18 November 2008

Available online 24 November 2008

Keywords:

Fe-mordenite

XRD

FTIR

Texturing

EDTA photodegradation

IC

ABSTRACT

Fe²⁺ was incorporated inside mordenite through ion exchange technique in aqueous solution. The amount of Fe loading was 25–100 wt %, using FeSO₄·7H₂O as precursor and Na-mordenite starting material Na-M. The Fe incorporated (Fe-M) thus prepared was characterized by XRD, FTIR and N₂ adsorption measurements. It was found that Fe mordenite retained the same structure as that for Na-mordenite which may indicate that Fe well dispersed into mordenite channels. BET indicated that Fe-M samples possessed higher surface area compared to the parent Na-M. Photocatalytic degradation of EDTA was carried out in presence of the prepared Fe-M catalysts. Effects of catalyst concentration and temperature were also studied. Thermodynamic parameters calculated for 50% Fe-M showed the highest catalytic activity toward EDTA degradation.

© 2008 Elsevier B.V. All rights reserved.

1. Introduction

In recent years zeolites are being extensively used in catalytic reactions [1]. There are many researches, where modifications in zeolite framework by introduction of some metal cations have been carried out in order to enhance their catalytic activity. Mordenite zeolite has been studied by XRD, IR, diffuse reflectance spectroscopy, surface area and water content [2]. The effect of Mo on the catalytic activity of HZSM-5 was studied during the conversion of methane into higher hydrocarbons and benzene [3]. In the initial period for the reaction of methane above 923 K complete oxidation of methane was the dominant process. However, after a partial reduction of the catalyst, the formation of several hydrocarbons was observed. The main products were benzene, ethylene and ethane. The selectivity to benzene was in the range of 60–70% at 1.2–6.3% methane conversion.

Gold encapsulated zeolites have been investigated by many researchers because of their catalytic activity toward many reactions [4,5]. It has been found that the Au⁺ forms the active sites which are responsible for the achievement of all reactions.

Recently, Fe loaded zeolites have attracted attention of many researchers especially in the field of environmental catalysis due to their activity and selectivity in many reactions such as a Photo-

Fenton reaction. It was found that, the incorporation of Fe into MCM-41 increased the catalytic activity of MCM-41 by about 60% for the photo-catalytic degradation of chlorinated phenols [6]. The catalytic activity of Fe incorporated zeolites was also investigated for photo-catalytic degradation of some different types of azo dyes [7]. The data indicate the enhancement of Fe modified zeolites activity by about 70%. Fe encapsulated inside zeolites may be located into two different sites (octahedral and tetrahedral) which lead to the formation of new active sites that are responsible for the improvement of adsorption properties of these types of catalysis especially for the removal of many organic pollutants [8].

The comparative study of the photocatalytic activity as heterogeneous catalysts of iron phthalocyanine (FePcs) supported on silica and/or encapsulated inside the cavities of zeolite Y have been established for the degradation of organic pollutants in aqueous and organic solution to cover wider range of possibilities. Differences in the extent of photochemical degradation in water or organic solvent phase arise from differences in solubilities of oxidant, including O₂ solubility, influence of pH, self-degradation, and ability of OH radical generation among other factors. Phenols are typical pollutants in aqueous medium that are recalcitrant to biological degradation. In addition, a standard protocol has been proposed in order to compare the activities of different photocatalysts based on their potential for degradation of phenol in water using Pyrex-filtered light [9–11].

* Corresponding author. Tel.: +20 106292802; fax: +20 222630677.

E-mail address: medhatmohamed@yahoo.com (M.M. El-Moselhy).

Table 1
The XRD unit cell parameters of mordenite (Na-M) and Fe-M catalysts.

Sample name	Cell constants Å			Cell volume Å ³	Cry. %	S _{BET} (m ² /g)	Fe content		
	a	b	c				Fe _f	Fe _{non f}	Fe ²⁺
Na-M	18.11	20.53	7.53	2798	100	340	–	–	–
25% Fe M	18.24	20.38	7.52	2795	90	378	0.73	0.92	0.23
50% Fe M	18.33	20.30	7.52	2798	86	416	1.7	2.3	0.85
75% Fe M	18.55	20.22	7.53	2823	82	485	3.4	4.8	0.65
100% Fe M	18.98	19.91	7.53	2852	77	564	5.2	6.8	0.35

Fe_f: framework iron, Fe_{non f}: non Framework iron, Cry: crystallinity.

It is well known that EDTA is one of the most common chelating agents that are used on a large scale in many industries. The removal of EDTA from waste water by using conventional techniques is not simple because it is not easily biodegradable and several recalcitrant compounds are formed during the degradation [12–17]. Methods based on the use of redox pair Fe (II/III) to destroy pollutants in water are increasingly reported. For example, Fenton's reagent is composed of a solution containing H₂O₂ and Fe²⁺ salts, in an acid medium. Fe³⁺ and Cu can also be used (Fenton-like reagents). The efficiency of the Fenton's reagent for destruction of organic matter can be enhanced by irradiation with light in the UV range; even solar light can be used [17–21].

The main objective of this study was to examine the influence of Fe loaded mordenite on the photo-degradation of EDTA. Fe was encapsulated inside mordenite in different percentages for improving the photo-degradability of EDTA which is one of the common organic pollutants

2. Experimental

2.1. Synthesis of Fe-M

The prepared Na-M [22] was stirred in aqueous solution of different FeSO₄ concentrations to give Fe loaded mordenite with 25, 50, 75 and 100 wt %. The samples were dehydrated in an oven overnight at 383 K and calcined at 823 K. The calcined samples were denoted as 25–100% Fe-M.

2.2. Characterization

The X-ray diffraction patterns of various zeolite samples were measured using a Philips diffractometer (type PW 1390). The diffraction patterns were run with Ni-filtered copper radiation ($\lambda = 1.5404 \text{ \AA}$) at 30 KV and 10 mA with a scanning speed of $2\theta = 2^\circ \text{ min}^{-1}$. The Fourier transform infrared (FTIR) spectra were recorded on a Bruker (Vector 22), single beam spectrometer with a resolution of 2 cm^{-1} .

Specific surface areas of various samples were obtained by the BET method at the liquid N₂ temperature (77 K) using a conventional volumetric apparatus. The samples were outgassed at 573 K for 3 h before measurement.

Total organic carbons (TOC) contents for EDTA before and after irradiation were measured using a Phoenix 800 Total carbon analyzer. UV–vis spectra of EDTA adsorbed on the photocatalyst before and after irradiation were measured using Cecil 7200 diffuse reflectance spectrometer at scanning speed 4000 nm/mm and a band width of 2 nm in the wavelength range from 190 to 250 nm. Concentrations of the degraded products were measured using ion chromatography (Dionex-pac) equipped with AS14 column with eluent consisted of 2:7 sodium carbonate: sodium bicarbonate mixture, and the flow rate was 1.2 ml/min.

2.3. Photocatalytic experiment

The photoreactivity experiments were carried out in a 200 ml cylindrical quartz glass reactor. Different EDTA concentrations

(0.0002–0.02 mol dm⁻³) were irradiated at room temperature (298 K). 0.02 mol dm⁻³ EDTA was degraded in presence of 50% Fe-M at different temperatures (298–318 K). In all cases, air was bubbled through the reaction mixture to maintain a constant dissolved O₂ concentration ($3 \times 10^{-4} \text{ mol dm}^{-3}$). A 6 W Hg lamp (254 nm) immersed within the photoreactor was used [7]. EDTA degradation was followed at different time intervals EDTA samples were taken out from the reaction mixture, filtered to remove any

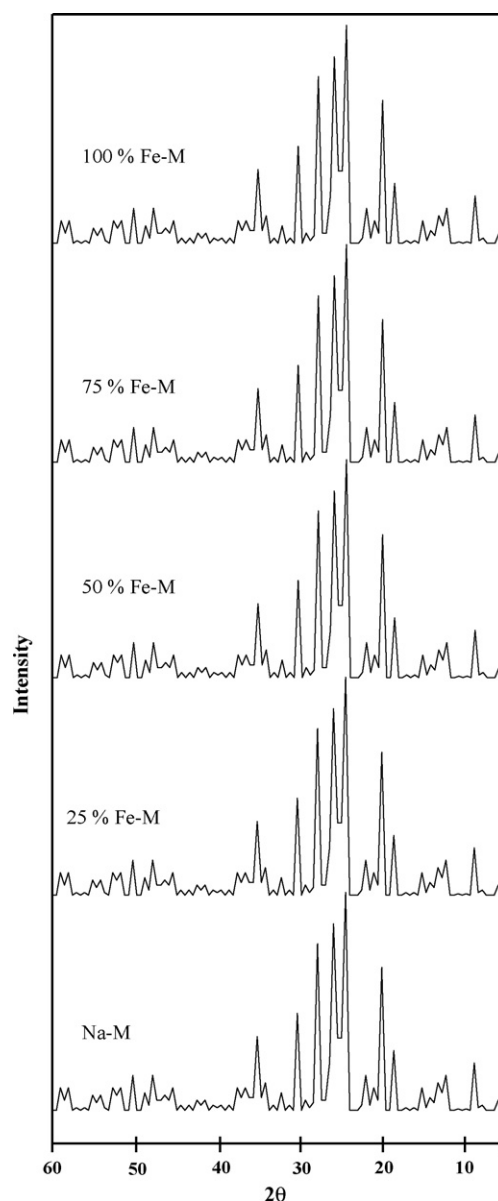


Fig. 1. X-ray diffraction patterns of the calcined Fe-M catalysts at varying loading of Fe (25–100 wt %) in comparison with the Na-M support.

dispersed zeolite and then quantified by complexometric titration with Mg^{+2} standard solution [23].

3. Results and discussion

3.1. Catalyst characterization

3.1.1. XRD of Fe-mordenite

The XRD results (Table 1) revealed that the Fe-containing mordenite samples exhibited typical lines of the Na-M zeolite, indicating that the structure of the zeolite remains intact after the treatment procedure. The observed decreases in the intensities

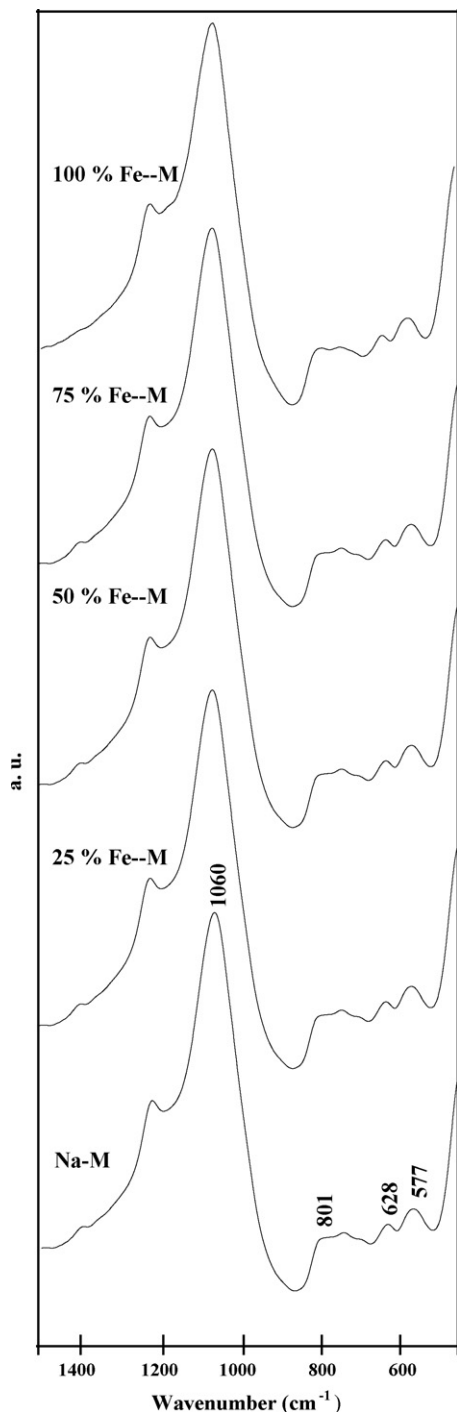


Fig. 2. FTIR spectra of Fe encapsulated mordenite at different concentrations.

of some samples correlated with the increasing Fe content of the samples. This decrease can be a result of the higher absorption coefficient of Fe compounds for the X-ray radiation and of the lower zeolite content in the samples [24]. Fig. 1 shows the absence of any diffraction line characteristic of Fe species as indicated in Fig. 1 suggests that the loaded Fe is finely dispersed inside mordenite channels.

The oxidation state of iron was examined using Mössbauer analysis. The data obtained show that the highest amount of Fe^{+2} was displayed by 50% Fe-mordenite Sample [8] if compared with the other samples as depicted in Table 1.

3.1.2. FTIR of Fe-mordenite

FTIR spectra of Fe-M (25–100 wt %) and of parent Na-M were depicted in Fig. 2 in comparison with the parent Na-mordenite. The data indicate that Fe-containing mordenite exhibit the same bands as those of Na-mordenite, indicating that Fe-mordenite retains the same zeolite structure as that of Na-mordenite even after the exchange process. The data also indicate the absence of any absorption band characteristic of any Fe species in the oxide form which may support that Fe was well incorporated into mordenite channels.

3.1.3. Surface area of Fe-M

Measurements of BET surface area (Figs. 3 and 4) of the Fe-M samples showed a marked increase in their total surface areas as compared to the parent Na-M, suggesting an integrity of the crystal structure as well as the absence of pore blocking by the

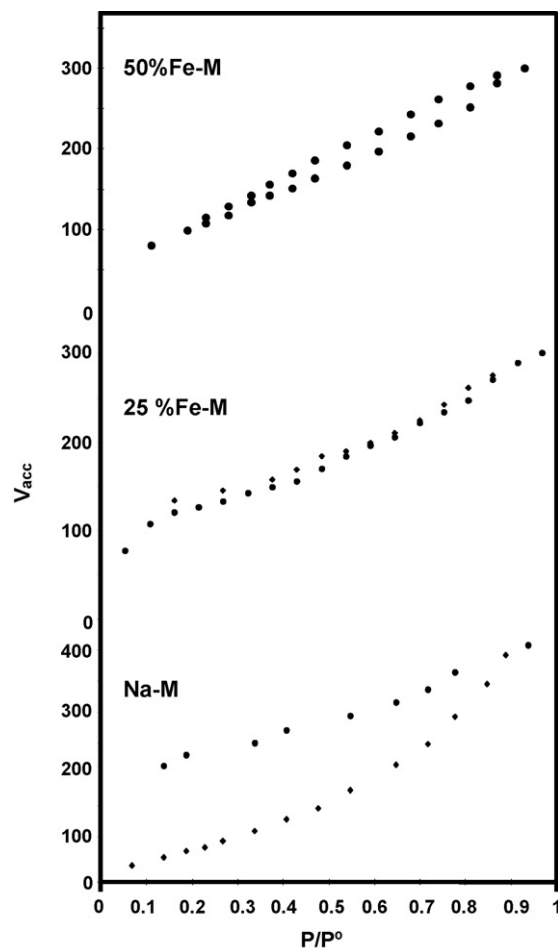


Fig. 3. Nitrogen adsorption–desorption isotherms at 77 K on Fe loaded Na-M samples (25 and 50 wt %) heated at 573 K.

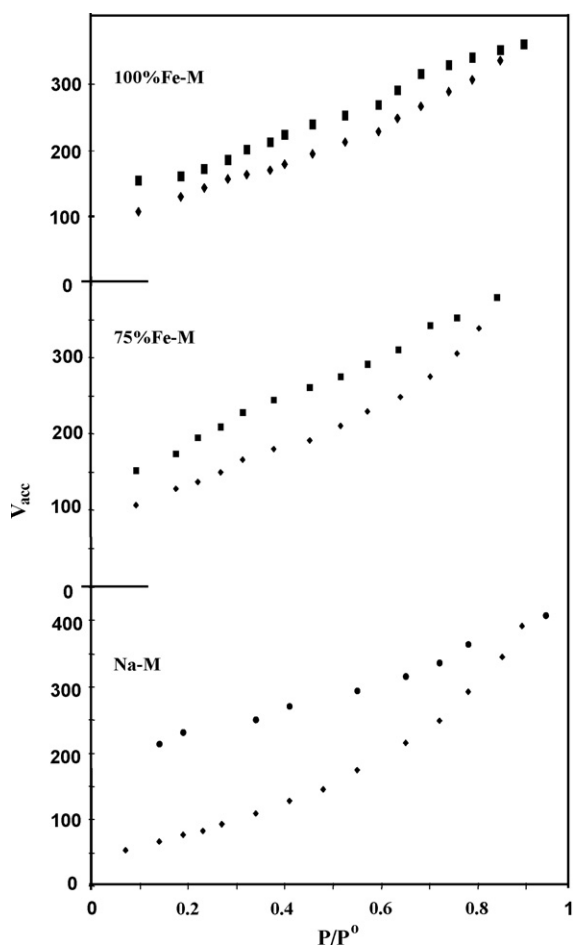


Fig. 4. Nitrogen adsorption–desorption isotherms at 77 K on Fe loaded Na-M samples (75 and 100 wt %) heated at 573 K.

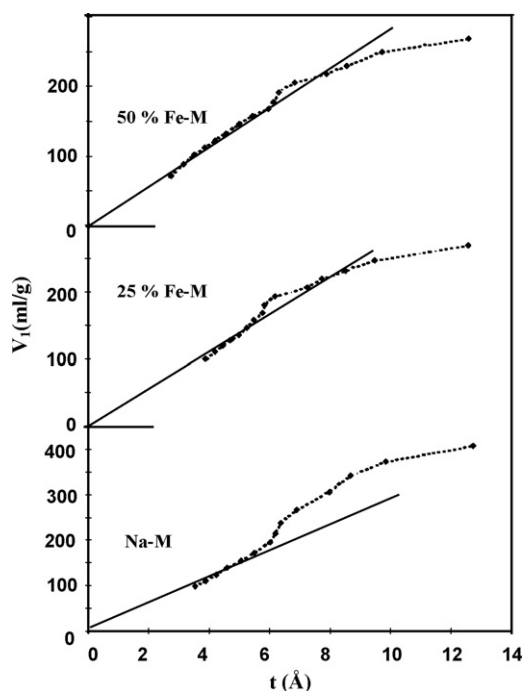


Fig. 5. V_{1-t} plots of different Fe loadings treated mordenite zeolite.

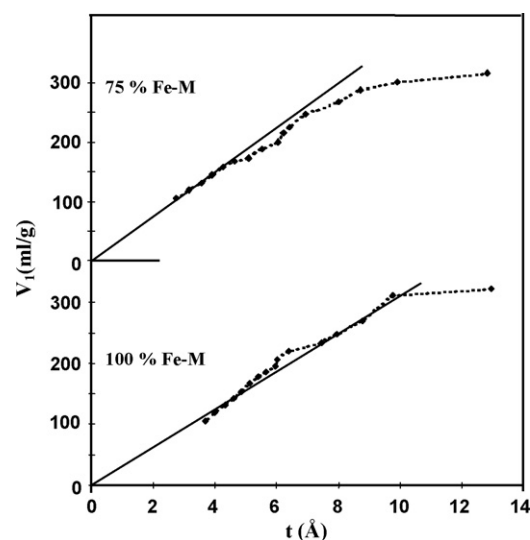


Fig. 6. V_{1-t} plots of different Fe loadings treated mordenite zeolite.

non-framework species. This is due to the adsorption of the highly dispersed iron oxide particles on the external surface of zeolite [8].

The obtained V_{1-t} plots of the parent Na-M (Figs. 5 and 6) show an upward swing starting at $t = 5.5 \text{ \AA}$ ($P/P^0 = 0.50$) and continuing up to $t \approx 12 \text{ \AA}$ ($P/P^0 = 0.90$) where it becomes nearly parallel (linear) indicating the domination of wide pores. The plot of 25% Fe-M sample exhibited a shrinkage in the upward swing if compared with the parent Na-M sample, indicating a partial blocking of the zeolite wide pores during the increase of the Fe contents. An upward deviation was also depicted for the 50% Fe-M sample implying that this sample indeed preserves wide pores. On the other hand, the V_{1-t} plot of the 75% Fe-M sample showed a downward deviation confirming the presence of narrow pores. The 100% Fe-M showed the resuming of wide pores; indicated by a limited upward deviation that ranging from 6.2 to 7.8 \AA .

3.2. Catalytic activity of Fe-M

Advanced oxidation process using Fe as a photocatalysts has been extensively investigated [1–7]. The process depends mainly on the formation of OH and can be explained as follows:

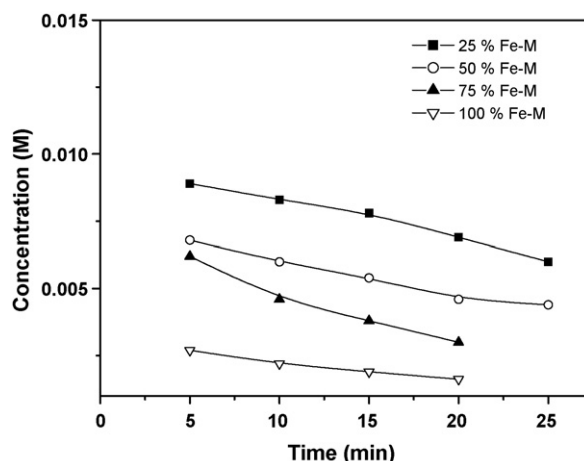


Fig. 7. EDTA adsorption over different Fe encapsulated mordenite.

The rate of reaction is governed by the amount of Fe^{2+} that reacts with H_2O to produce OH radicals. The advantages of zeolite modification with Fe and its using as a photocatalyst:

1. higher surface area
2. higher Fe content
3. catalyst recovery and reuse

3.2.1. Adsorption of EDTA

Since the rate of most catalytic reactions generally depends on the amount of adsorbed molecules, a series of experiments were carried out in the dark to study the adsorption of EDTA on Fe-mordenite surface with different Fe-M types (25–100%). It was found that the equilibrium adsorption was reached in less than 30 min.

The adsorption kinetics of EDTA molecules (or its rate of disappearance from solution phase) on 4 catalysts with different Fe loadings are shown in Fig. 7. The results indicated that all adsorption isotherms are linear with all catalysts. The plot also indicates that the slope of linear isotherm decreases in 100% Fe-M sample. From this observation it may be concluded that the extent of adsorption of EDTA molecules decreases as the concentration of loaded iron increases.

3.2.2. EDTA degradation

3.2.2.1. UV irradiation. Different initial concentrations of EDTA solutions were subjected to UV irradiation (254 nm) under a constant flow of oxygen. The data obtained indicate that EDTA was

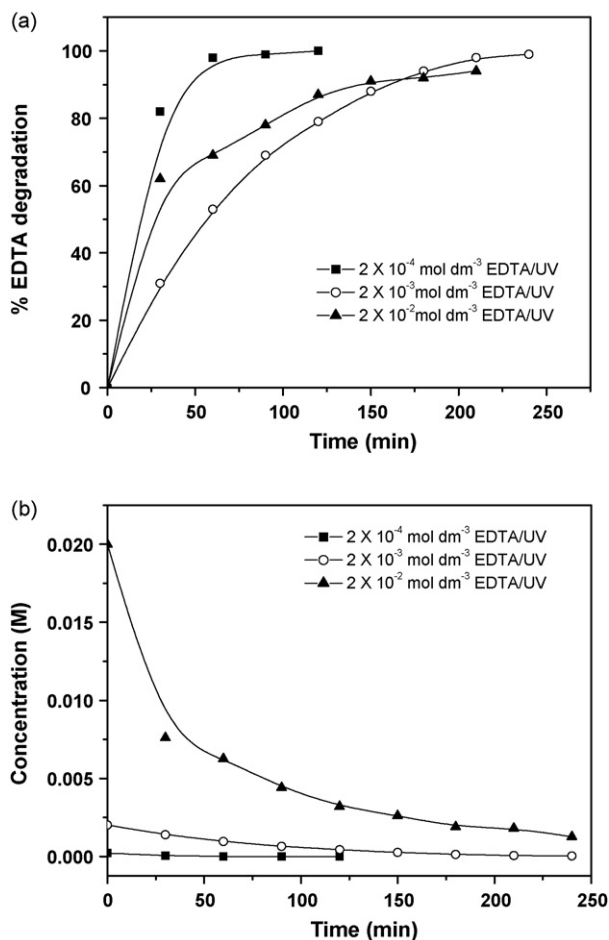


Fig. 8. (a) % degradation of EDTA versus time and (b) different concentrations versus time for degradation of EDTA.

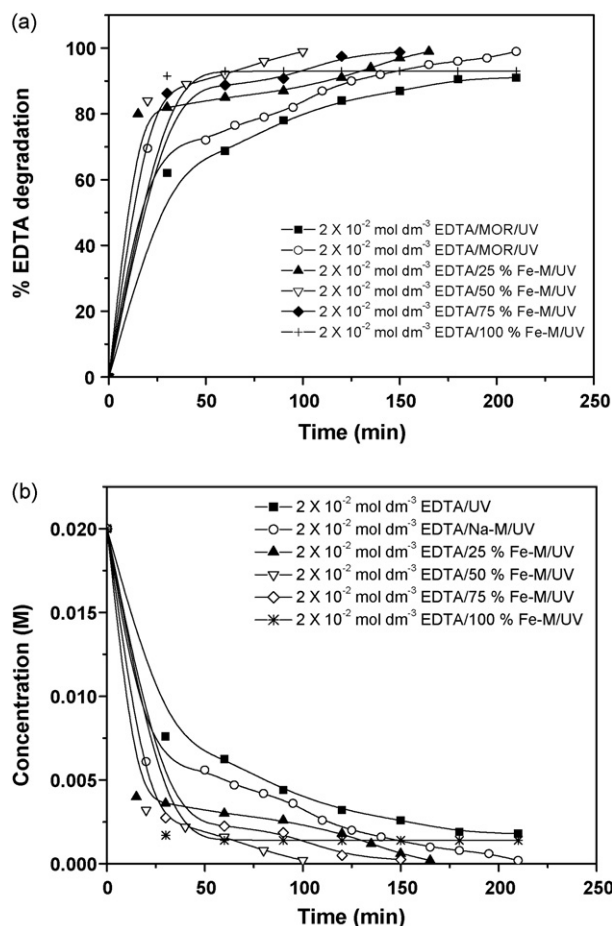


Fig. 9. (a) % degradation of EDTA versus time over different Fe encapsulated mordenite and (b) different concentrations versus time for degradation of EDTA over different Fe encapsulated mordenite.

degraded under the influence of light only, but degradation requires a large time as depicted in Fig. 8. The percentage of degradation was varied from 92 to 100% depending on the concentration of EDTA used.

3.2.2.2. Effect of catalyst. Aqueous suspensions of 25–100% Fe-M (0.2 g L^{-1}) containing 2 mM EDTA were irradiated under UV light for different illumination times, and samples were taken periodically for analysis after stirring for about 30 min to attain the equilibrium. The obtained data show that Fe-M had a great influence on the degradation process if compared with Na-M (Fig. 9). It was found that, the initial rate of degradation was very fast due to the adsorption of EDTA on the catalyst surface at the start of degradation reaction with respect to all samples. The extent of degradation reaches 100% with all samples but at different periods of time except 100% Fe-M which shows a different behavior because the degradation reaction was stopped after 60 min from the start of irradiation. It is clear that, the increase of iron loading into mordenite increases the rate of degradation of EDTA and this may be due the formation of new active sites created upon the dispersion of iron species (Fe^{2+} and Fe^{3+}) on the surfaces of mordenite which improve the activity toward photodegradation processes. Despite 100% Fe-M sample containing large amount of incorporated iron, it showed the lowest EDTA degradation this may be due to this that the sample possesses a lower Fe^{2+} content (Table 1) which plays an important role in the process of degradation. As the amount of incorporated iron increase, this increases the amount of leached iron (non-framework) as depicted in Table 1 which may react with

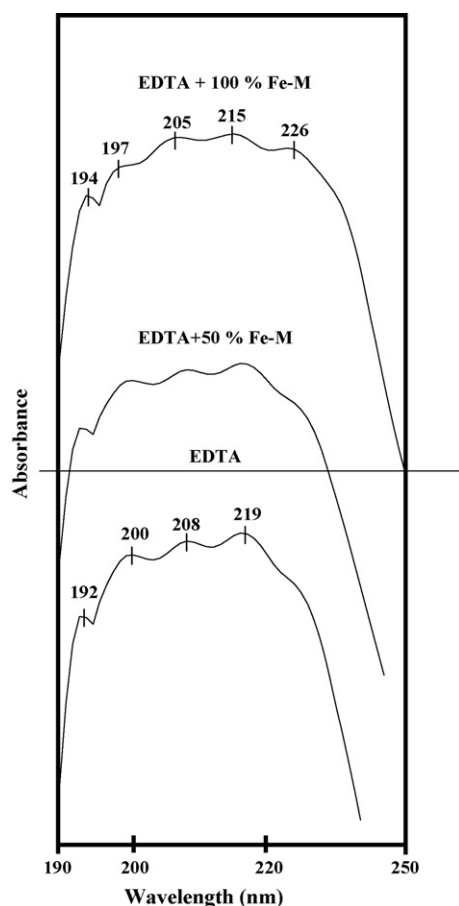


Fig. 10. UV-vis spectra of adsorbed EDTA on the catalyst surface in comparison with those of EDTA itself.

EDTA to $\text{Fe}^{\text{III}}(\text{EDTA})$ complex which upon exposure to UV reacts with water and gives OH groups and prevents the formation of OH radicals which accelerate the process of degradation (see the proposed mechanism). The formed Fe-Chelate was not affected by UV irradiation, so the degradation process did not come to the end.

Fig. 10 shows the UV-vis spectra of EDTA adsorbed on the catalyst surface for two samples (50 and 100% Fe-M) in comparison with that of EDTA. It is clear that a small shift toward lower wavelength takes place after the adsorption of EDTA on the surface of 100% Fe-M sample. This shift may be due to the combination of adsorbed EDTA with any cationic species on the surface of the catalyst. The figure also indicates the appearance of a new absorption band at 226 nm which may be assigned to formation of Fe-EDTA complex [25,26] which supports the inactivity of this sample. On the other hand, the spectrum of EDTA adsorbed on the surface of 50% Fe-M (Fig. 10) exhibits the same absorption bands (192, 200, 208 and 219 nm) as that of EDTA indicating that the amount of free Fe on the catalyst surface is very small and/or completely absent which may indicate that Fe dispersed inside mordenite channels. Furthermore, the later sample possesses a higher Fe^{2+} content when compared with the former one (Table 1).

The results of % TOC obtained for EDTA degradation illustrate that, for all samples (25–75% Fe-M) the removal of TOC is very high at the end of reaction. Especially 50% Fe-M samples which show the highest TOC removal capacity. The lower TOC decrease is consistent with the lower activity of the 100% Fe-M sample in inducing the degradation of EDTA.

The effects of catalyst concentration on the degradation process were investigated by using three different Fe-M concentrations (0.05, 0.10 and 0.15 g/100 ml EDTA solution). Fig. 11 shows the effect

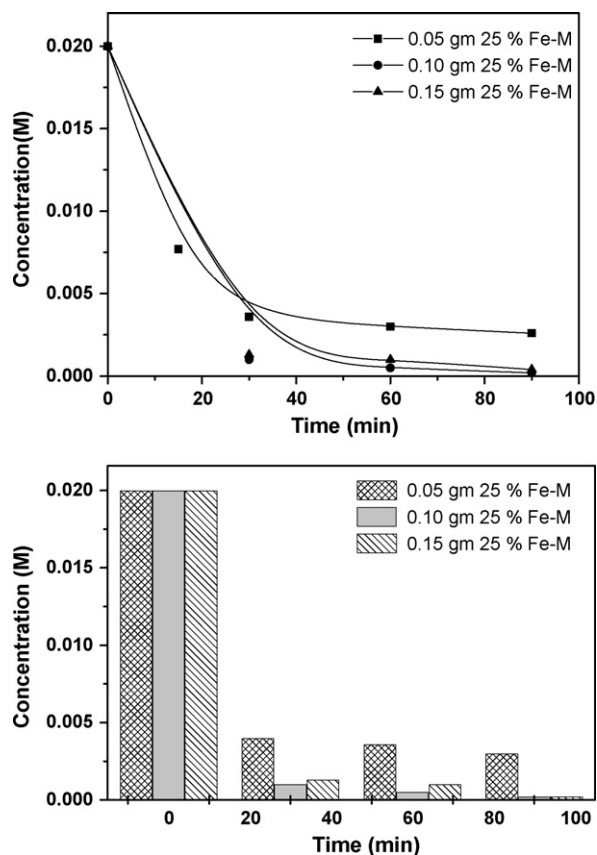


Fig. 11. Effect of catalyst concentration on the photocatalytic degradation of EDTA solution.

of varying Fe-M amount on the degradation of EDTA. The data indicate that the rate of degradation increases with the increase of Fe-M dosage until a certain limit beyond which no effect will happen.

One important consideration in photodegradation reactions is to calculate the order of reaction and rate constant to get a simple clue about the role of the catalyst in the reaction. Fig. 12 shows a plot of $\ln C/C_0$ versus time for EDTA degradation on different iron loaded mordenite catalysts. It is clear that all reactions follow first order kinetics and the calculated apparent rate constants indicate that 50% Fe-M is the most effective sample for the removal of EDTA

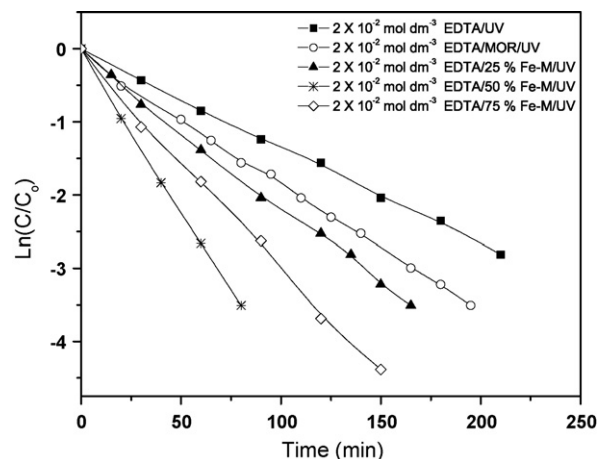


Fig. 12. $\ln(C/C_0)$ versus time for photocatalytic degradation of EDTA over 25–75% Fe encapsulated mordenite.

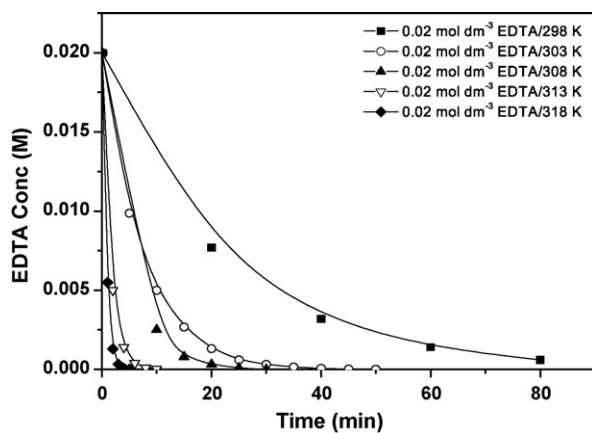


Fig. 13. Photocatalytic degradation of EDTA over 50 Fe encapsulated mordenite at different temperatures.

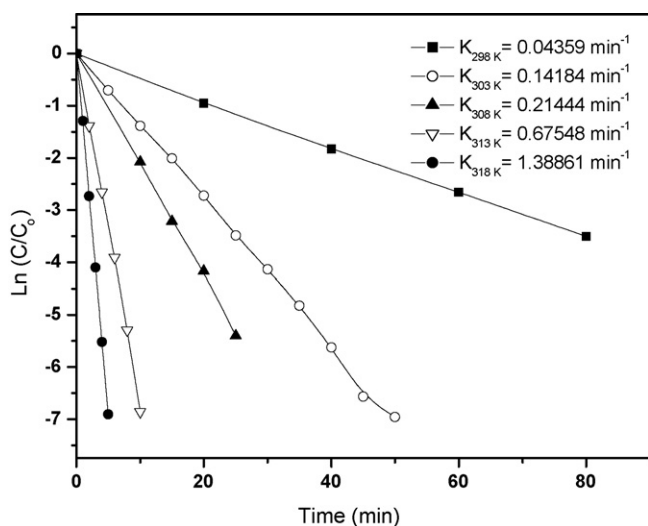


Fig. 14. $\ln(C/C_0)$ versus time for photocatalytic degradation of EDTA over 50% Fe encapsulated mordenite at different temperatures.

which may be assigned to the highest amount of Fe^{2+} possessed by this sample that plays an important role in the formation of OH radicals.

To investigate the effect of temperature on the reaction pathway the reaction mixture was transferred to a thermostat adjusted at the target temperature and the obtained results are represented in Figs. 13 and 14. It is clear that, temperature has a great effect on the reaction rate. Furthermore, increase in temperature leads to the increased mobility of EDTA molecules and accelerates the adsorption–desorption rate of both EDTA and the degradation products and this increases the uncovered surface to a new reacted molecules.

\ln of the obtained rate constants were plotted against $1/T$ (Fig. 15) and the calculated thermodynamic parameters are reported in (Table 2). The obtained ΔG^\ddagger and the negativity of the

Table 2
Thermodynamic parameters of EDTA degradation over 50% Fe-M.

$T(K^\circ)$	$\ln K$	ΔG^\ddagger KJ/mol	ΔH^\ddagger KJ/mol	ΔS^\ddagger Joule/deg. mol	$T\Delta S^\ddagger$ J/K mol
298	-3.1329	7.7489	0.1355	-25.55	-7.61
303	-1.9531	4.9119	0.1355	-15.76	-4.78
308	-1.5397	3.9361	0.1355	-12.34	-3.80
313	-0.3923	1.0192	0.1355	-2.82	-0.88
318	+0.3283	-0.8665	0.1355	+3.15	+1.00

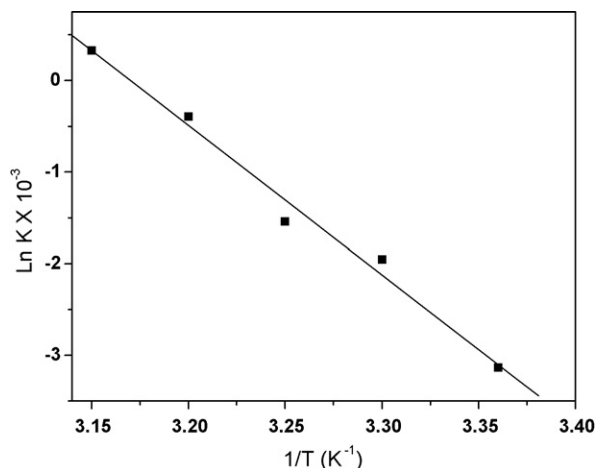


Fig. 15. $\ln K$ versus $1/T$ for photocatalytic degradation of EDTA over 50% Fe encapsulated mordenite at different temperatures.

obtained ΔS^\ddagger and positivity of ΔH^\ddagger mean that the photocatalytic degradation of EDTA cannot be spontaneous at any temperature. The data also imply that the calculated activation energy of this reaction is extremely low ($\Delta E = 8.23 \text{ cal K}^{-1} \text{ mol}^{-1}$).

Fig. 16.

Through chromatographic analysis the following intermediates and products were detected after photocatalytic runs of different duration: formic, oxalic, oxamic, glyoxylic and glycolic acids, IMDA, Gly, ammonium and EDA. Formaldehyde was also qualitatively detected, but not quantified. Nitrate and nitrite were also detected.

According to the accepted mechanism for heterogeneous photocatalytic processes, OH radicals are generated after absorption of light. Organic compound can be oxidized directly by hydroxyl radicals. Taking into account the identity and amount of products detected in our experiments, in conformity with the previously proposed mechanisms with other oxidants [27–30], we hypothesize that photocatalytic degradation of EDTA with Fe-M proceeds through three possible pathways (A), (B) and (C). Depending upon the point of attack of OH radicals to the molecule, ED3A or IMDA or glyoxylic acid can be formed in the initial step (Scheme 1). Successive OH radicals attacks, combined with other dark processes, induce step by step cleavage of EDTA forming intermediates indicated in Scheme 1, together with CO_2 , CH_2O and NH_4^+ . Formaldehyde is further oxidized

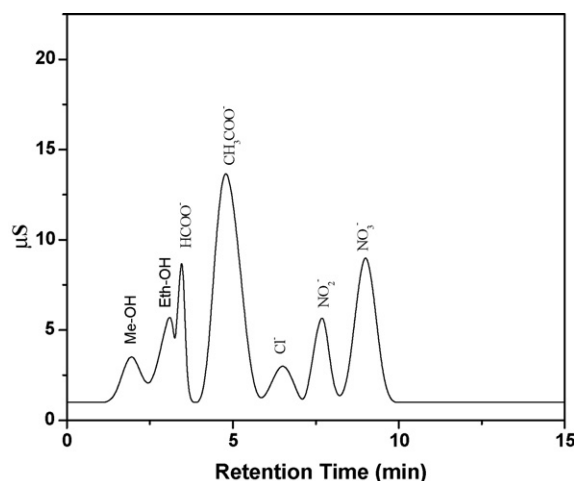
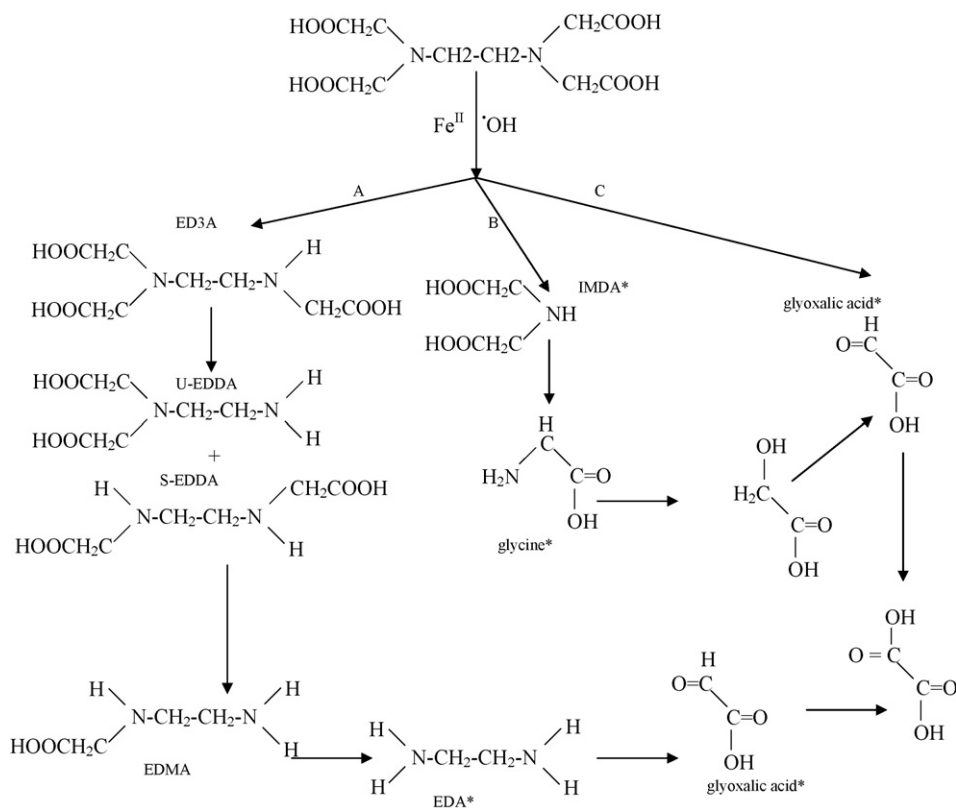


Fig. 16. IC chromatogram of EDTA after photodegradation on 50% Fe-M catalyst.



Scheme 1.

to formic acid. IMDA is decomposed to Gly, which is known to transform slowly to oxamic acid [30], and this explains why this compound cannot be seen during the initial stages of the reaction. Glyoxylic acid is further oxidized to oxalic and/or formic acids.

4. Conclusion

The process of mordenite modification with Fe cations was found to increase the total surface area of mordenite depending on the amount of loaded Fe. The examination of the Fe modified mordenites in photo-degradation of EDTA shows that the highest catalytic activity was observed for 50% Fe-M. The increase of Fe loading did not indicate any significant activity. Investigation of the effect of temperature was found to greatly affect the rate of EDTA degradation.

Acknowledgments

This research has been carried out in the Science Center for Detection and Remediation of Environmental Hazards (SCDREH), Al-Azhar University. Most of the measurements have been carried out in Faculty of Science, Chemistry Department, Al-Azhar University and El-Tebben Institute-Helwan, Egypt.

References

- [1] R.M. Mohamed, A.A. Ismail, I. Othman, I.A. Ibrahim, J. Mol. Catal. A; Chem. 238 (2005) 151–157.
- [2] R. Cid, F.J. Gileambias, J.L.G. Fierro, A.L. Agudo, J. Villasenor, J. Catal. 89 (1984) 478.
- [3] A.S.F. Solymosi, Appl. Catal. A, General 145 (1996) 361.
- [4] M.M. Mohamed, T.M. Salama, M. Jchikawa, J. Colloid. Interface Sci. 228 (2000) 175.
- [5] M.M. Mohamed, M. Jchikawa, J. Colloid. Interface Sci. 232 (2000) 381.
- [6] M. M. El-Moselhy; Ph. D. Thesis, Chemistry Department, Faculty of Science, Al-Azhar University, 2004.
- [7] M.M. Emara, A.M.S. Tourky, M.M. El-Moselhy, Eg. J. Chem. 49 (2) (2008) 241–259.
- [8] M.M. Mohamed, N.S. Gomaa, M. El-Moselhy, N.A. Essa, J. Colloid. Interface Sci. 259 (2003) 331–337.
- [9] N. Serpone, A. Salinaro, Pure Appl. Chem. 71 (1999) 303–320.
- [10] A. Salinaro, A.V. Emeline, J. Zhao, H. Hidaka, V.K. Ryabchuk, N. Serpone, Pure Appl. Chem. 71 (1999) 32.
- [11] M. Alvaro, E. Carbonell, M. Espla, H. Garcia, Appl. Catal. B: Environ. 57 (2005) 37–42.
- [12] D.W. Sundstrom, J.S. Allen, S.S. Fenton, F.E. Salimi, K.J. Walsh, Treatment of Chelated iron and copper wastes by chemical oxidation, J. Environ. Sci. Health A 31 (1996) 1215–1235.
- [13] P.A. Babay, C.A. Emilio, R.E. Ferreyra, E.A. Gautier, R.T. Gettar, M.I. Litter, Kinetics and mechanisms of EDTA photocatalytic degradation with TiO₂ under different experimental conditions, Int. J. Photoenergy 3 (2001) 193–199.
- [14] M. Sorensen, F.H. Frimmel, Photochemical degradation of hydrophilic xenobiotics in the UV/H₂O₂ process: influence of nitrate on the degradation rate of EDTA, 2-amino-1-naphthalenesulfonate, diphenyl-4-sulfonate and 4,4'-diaminostilbene-2,2'-disulfonate, Water Res. 31 (11) (1998) 2885–2891.
- [15] J.K. Yang, A.P. Davis, Photocatalytic oxidation of Cu (II)-EDTA with illuminated TiO₂: kinetics, Environ. Sci. Technol. 34 (17) (2000) 3789–3795.
- [16] P.A. Babay, C.A. Emilio, R.E. Ferreyra, E.A. Gautier, R.T. Gettar, M.I. Litter, Kinetics and mechanisms of EDTA photocatalytic degradation with TiO₂, oxidation technologies for water and waste water treatment (II), Water Sci. Technol. 44 (5) (2001) 179–185.
- [17] G. Ghiselli, W.F. Jardim, M.I. Litter, H.D. Mansilla, J. Photochem. Photobiol. A; Chem. 167 (2004) 59–67.
- [18] A. Safarzadeh-Amiri, J.R. Bolton, S.R. Cater, Ferrioxalate-mediated solar degradation of organic contaminants in water, Solar Energy 56 (5) (1996) 439–443.
- [19] A. Safarzadeh-Amiri, J.R. Bolton, S.R. Cater, Ferrioxalate-mediated solar degradation of organic pollutants in contaminated water, Water Res. 31 (4) (1996) 787–798.
- [20] J.J. Pignatello, Dark and photoassisted Fe³⁺-catalyzed degradation of Chlorophenoxy herbicides by hydrogen peroxide, Environ. Sci. Technol. 26 (1992) 944–951.
- [21] S.H. Bossmann, E. Oliveros, S. Gob, S. Siegwater, E.P. Dahlem, L. Payawan, M. Straub, M. Worner, A.M. Braun, New evidence against hydroxyl radicals as reactive intermediates in the thermal and photochemically enhanced Fenton reaction, J. Phys. Chem. A 102 (1998) 5542–5550.
- [22] M.M. Reda, A.M. Hisham, E.F. Mohamed, I.A. Ibrahim, Microporous Mesoporous Mater. 79 (2005) 7.

- [23] C.W. Schaper, N.N. Vlasova, S.K. Poznyak, A.I. Kokoring, *J. Collod. Interface Sci.* 239 (2001) 200.
- [24] M. M. El-Moselhy, Master Thesis, Al-Azhar University, 2001.
- [25] G. Anderegg, *Critical Survey of Stability Constants of EDTA Complexes*, Pergamon Press, Oxford, 1977.
- [26] A. Ringbom, *Complexation in Analytical Chemistry*, Wiley, New York, 1963.
- [27] E. Gilbert, S. Hoffmann-Glewe, *Water Res.* 24 (1990) 39.
- [28] M. Sørensen, Dr.-Ing. Thesis, Faculty of Chemical Engineering, Fridericiana Karlsruhe University, (1996).
- [29] M. Sørensen, S. Zurell, F.H. Frimmel, *Acta Hydrochim. Hydrobiol.* 26 (1998) 109.
- [30] D. Chen, A.E. Martell, D. McManus, *Can. J. Chem.* 73 (1995) 264.